Geophysical Journal International

Geophys. J. Int. (2011) **186,** 1029–1035 doi: 10.1111/j.1365-246X.2011.05121.x

Low temperature magnetic behaviour near 35 K in unmetamorphosed claystones

Myriam Kars,[1,2] Charles Aubourg[1] and Jean-Pierre Pozzi[2]

[1]*Laboratoire des Fluides Complexes et leurs Réservoirs* (UMR 5150), *Université de Pau et des Pays de l'Adour, Avenue de l'Université,* 64013 *Pau cedex, France. E-mail: kars@geologie.ens.fr*

[2]*Laboratoire de Géologie, CNRS* (UMR 8538), *Ecole Normale Supérieure,* 24 *rue Lhomond,* 75231 *Paris cedex* 05, *France*

Accepted 2011 June 22. Received 2011 May 20; in original form 2010 July 27

SUMMARY

There is growing evidence that the magnetic assemblage of claystones, illustrated by low-temperature magnetic transitions at ∼120 K and ∼35 K, may be representative of the peak burial temperature in the so-called oil-window (60–150°C). In previous studies, it was proposed that this magnetic assemblage is characterized by fine-grained pyrrhotite (Fe_7S_8) and magnetite (Fe_3O_4). However, evidence of pyrrhotite was not so obvious and the magnetic transition near 35 K of fine-grained pyrrhotite has similarities with those of siderite ($FeCO_3$) or rhodochrosite ($MnCO_3$). Here, we propose some diagnostic tests to distinct <50 K behaviours by studying claystones from Netherlands borehole and Borneo Prism that experienced different peak burial temperatures. We perform magnetic susceptibility, temperature dependency of SIRM (ZFC, RT-SIRM) and field cooled hysteresis loops. On cooling of RT-SIRM (300 K to 10 K), we applied a magnetic field of 5 μT to enhance Néel type magnetic transition. It is found that our samples can be classified in two categories based on the shape of the RT-SIRM curve: one displaying an abrupt break-in-slope in the remanence at ∼30 K, called *N*-behaviour, and the other one characterized by a progressive increase of the remanent magnetization by 80 K, named *P*-behaviour. The first category contains essentially magnetite and Fe–Mn carbonates, the second one magnetite and probably iron sulphides.

Key words: Magnetic and electrical properties; Rock and mineral magnetism; Phase transitions.

1 INTRODUCTION

Claystones are potentially oil source rocks in sedimentary basins and thrust belts. Aubourg & Pozzi (2010) proposed recently that a given magnetic assemblage of claystones may be diagnostic of burial within the oil window from 60°C to 150°C (Sweeney & Burnham 1990). More precisely, they proposed that fine-grained pyrrhotite (Fe_7S_8) and magnetite (Fe_3O_4) formed from 2 km depth and more. Thus, the occurrence of these two magnetic minerals may inform on the maturity of claystones. To define the magnetic assemblage in rocks where organic matter coexists with iron sulphides, the best way is certainly low temperature investigation (<300 K; <27°C) because it prevents the chemical transformation, which arises from heating higher than room temperature usually used in palaeomagnetic studies (Van Velzen & Zijderveld 1992). Stoichiometric magnetite is firmly identified by a magnetic transition at 120 K, named Verwey transition (e.g. Ozdemir *et al*. 2002). This transition results from a solid-state phase change from cubic above 120 K to monoclinic below 120 K (e.g. Muxworthy & McClelland 2000; Walz 2002). Pyrrhotite is characterized by a magnetic transition at 35 K and its origin remains unknown (Dekkers *et al*. 1989; Rochette *et al*. 1990). When the saturation isothermal remanent magnetization (SIRM) is cooled down from 300 K to 10 K, the pyrrhotite transition for grains larger than 1 μm is marked by a loss of remanence. Its recovery on warming is an indication of domain state, and therefore grain size (Dekkers *et al*. 1989). Instead of a regular pyrrhotite transition, Aubourg & Pozzi (2010) reported a peculiar magnetic behaviour at ∼35 K during the cooling of RT-SIRM, named hereafter the *P*-behaviour. More precisely, they showed that the *P*-behaviour of Opalinus claystones from the Jura fold belt is a combination of an induced magnetization and a pyrrhotite transition. Both are detected at ∼35 K, which led Aubourg & Pozzi (2010) to propose that the *P*-behaviour is due to the input of fine-grained pyrrhotite. However, evidence of pyrrhotite in the samples is not so clear. Besides, rhodochrosite ($MnCO_3$, Néel temperature $T_N = 32$ K; Kosterov *et al*. 2006), siderite ($FeCO_3$, $T_N = 38$ K; Housen *et al*. 1996) and lepidocrocite (γ-FeOOH, $T_N = 52$ K; Hirt *et al*. 2002) are likewise candidates to explain the origin of this behaviour. Rhodochrosite and siderite (Frederichs *et al*. 2003) can occur in solid solution because Fe^{2+} and Mn^{2+} can easily substitute each other, leading to Néel temperatures ranging from 32 to 38 K. In this study, our aim was to add new low temperature data to characterize the nature of the *P*-behaviour. The different magnetic measurements, performed on four samples coming from two different sites, permitted to classify these specimens in two categories: one shows a characteristic Néel transition and the other one displays a *P*-behaviour.

2 SAMPLES AND METHODS

Work in progress of claystones from different boreholes and the Borneo accretion prism reveals a homogenous pattern of low-temperature rock magnetic properties. We have selected four representative claystones from a set of tens of samples. We studied two claystones from a borehole in the Netherlands (samples A and B) and two claystones from the Borneo Eocene prism (samples C and D). Sample A is a calcareous claystone. The samples A and B are located at 1538 m and 1793 m depth, respectively (depth interval 255 m). There is a Cretaceous–Carboniferous unconformity at 1597 m depth between sample A (Cretaceous) and sample B (Carboniferous). This involves different burial history for sample B. Maturity parameters from vitrinite reflectance are Ro = 1.4 per cent and Ro = 1.8 per cent for A and B, respectively (unpublished report). However, regarding the basin history, it is likely that the sample A vitrinite reflectance is <1 per cent. The samples C and D are taken in the Crocker formation from the Sarawak prism from two road-cut fresh outcrops (Sapin *et al*. 2011). The maturity parameters of sample C and D are Ro = 0.7 per cent and Ro = 1.2 per cent, respectively. Regarding vitrinite data, Borneo and Netherlands samples are early mature (A, C; burial temperature $T_{bu} < 120^{\circ}$C) to overmature (B, D; $T_{bu} > 150^{\circ}$C; Sweeney & Burnham 1990).

We measured the magnetic properties of the four claystones at the Institute for Rock Magnetism, University of Minnesota, Minneapolis, USA. We studied the temperature dependency in the range 300 K-10 K of SIRM. For this purpose, we used the following measurement cycle:

(1) a 2.5 T field was applied at 300 K to impart an Isothermal Remanent Magnetization (IRM) and then switched off. The samples were cooled down to 10 K within an upward magnetic field of 5 μT (∼1/10 of the Earth's magnetic field) at about 5 K steps. This part of the measurement cycle is called RT-SIRM (RT for Room Temperature). The application of a magnetic field of 5 μT inside the MPMS (controlled by a fluxgate) was proposed by Aubourg & Pozzi (2010) with the aim to exacerbate the amplitude of the *P*-behaviour below 100 K. Generally, the cooling of a RT-SIRM is performed under a trapped magnetic field lower than 0.1 μT. For convenience, we will talk about remanence monitoring, while in fact, this is a monitoring of a RT-SIRM and a small induced magnetization, which parallels the magnetic field of 5 μT. We have now the practice of tens of measurements in claystones using this procedure. Despite the paramagnetic input of clays, this procedure allows the detection of Néel transitions that are not visible using the zero-field cooling of a RT-SIRM.

(2) at 10 K, LT-SIRM was imparted with a 2.5 T magnetic field. Then, the magnetic field is switched off. The samples were warmed back to 300 K in zero field at 10 K steps. This is called Zero Field Cooled (ZFC).

We studied the temperature dependency of AC magnetic susceptibility from 300 K to 10 K. We obtained from this measurement the in-phase magnetic susceptibility (K') and the quadrature (out-of-phase) magnetic susceptibility (K''). Magnetic susceptibility was measured at different magnetic field strength (from 16 to 240 A m^{-1}) at 100 Hz. RT-SIRM, ZFC, K′ and K″ were measured using two Quantum Design Magnetic Properties Measurement System (MPMS). We studied the hysteresis loops using a Princeton Vibrating Sample Magnetometer (VSM). We ran hysteresis loops at room temperature and at low temperature (<100 K). The samples were cooled from 300 K to 10 K in a field of 1 T to impart a field-cooled remanence (FC). All magnetic measurements (MPMS and VSM) were done on samples powders of about 400 mg sealed in a gel capsule.

3 RESULTS

At room temperature, the low field magnetic susceptibilities (K_{lf}) for samples A, B, C and D are 120, 641, 349 and 309 μSI, respectively (Table 1). The ferromagnetic susceptibility ($K_{ferro} = K_{lf} - K_{hf}$), inferred from the high-field magnetic susceptibility (K_{hf}), represents 30–40 per cent of the low-field magnetic susceptibility (Table 1). SIRM are 56, 105, 140 and 42 μAm^2 kg^{-1} for samples A, B, C and D, respectively. SIRM and K_{ferro} values indicate a weak concentration of ferromagnetic minerals. ZFC and RT-SIRM demagnetization curves are shown in Fig. 1, together with the derivatives from 10 to 50 K shown in inset. ZFC demagnetization curves (Fig. 1a, c), when plotted in a log-scale, are characterized by a 2-step pattern, with: (1) a large drop of LT-SIRM between 10 and 35 K (a minimum of 80 and a maximum of 99 per cent of the remanence are lost), and (2) a change-in-slope at 120 K which is characteristic of stoichiometric magnetite.

RT-SIRM demagnetization curves (Fig. 1b, d) show that all claystones display the Verwey transition at 120 K, in agreement with the ZFC demagnetization curves. Below 120 K, the behaviour of the magnetization is different. For claystone C, the magnetization increases regularly from ∼100 K to 10 K (see inset Fig. 1d). The claystone A presents also an increase in the same range of temperature, but a break-in-slope is apparent at ∼30 K (see inset Fig. 1b). The claystones B and D display an abrupt magnetic transition at ∼40 K and ∼30 K, respectively (see inset Fig. 1b, d). The magnetization parallels the 5 μT magnetic field applied upward. Samples A and C present a regular increase of RT-SIRM from 70–80 K to 10 K. Sample C is also characterized by a progressive rise of the magnetization from 300 K to the Verwey transition temperature. Sample B reveals a slightly concave curve around 40–50 K and then a sharp increase from 38 K, before being convex from 25 to 10 K. Sample D magnetization is quasi-constant from room temperature to 120 K, where a drop is observed, and again remains constant to 30 K. At this temperature, a sharp upward break-in-slope is observed with a slight decrease at very low temperature.

We show FC hysteresis loops after slope correction obtained between 10 and 50 K (Fig. 2). Claystones A and C display hysteresis

Table 1. Some rock magnetic properties at room temperature for the four claystones. X_{lf}: low field magnetic susceptibility. X_{hf}: high-field magnetic susceptibility. X_{ferro}: ferromagnetic susceptibility ($X_{ferro} = X_{lf} - X_{hf}$). M_s and M_{rs}: magnetization at saturation and remanence at saturation. H_c and H_{cr} coercive magnetic field and back remanence coercive field. All parameters, but X_{lf}, are measured with a vibrating sample magnetometer.

Sample	X_{lf} (μSI)	X_{hf} (μSI)	X_{ferro} (μSI)	M_s (μAm^2 kg^{-1})	M_{rs} (μAm^2 kg^{-1})	H_c (mT)	H_{cr} (mT)
A	120	71	49	485	68	10	39
B	641	430	211	2460	135	17	39
C	349	214	135	1267	124	13	34
D	309	216	93	574		8	36

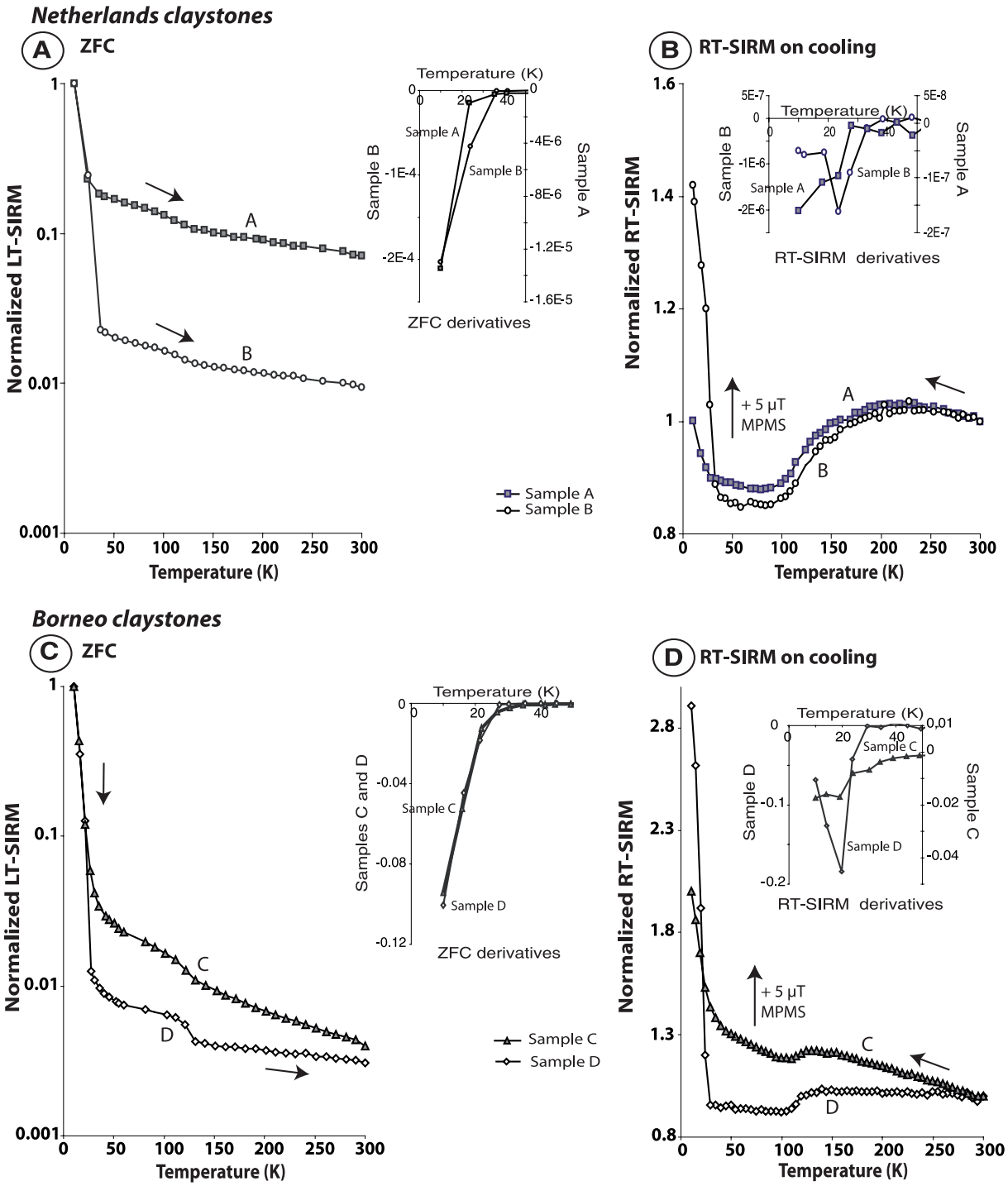

Figure 1. MPMS measurements in the 10–300 K temperature range. For the Netherlands samples: (a) Zero Field Cooled (ZFC) curve from 10 K to 300 K and (b) RT-SIRM on cooling from 300 K to 10 K and for Borneo samples: (c) Zero Field Cooled curve from 10 K to 300 K and (d) RT-SIRM on cooling from 300 K to 10 K.

loops with weak coercivity (Fig. 2a, c) less than 15 mT at 10 K. The behaviour of claystones B and D is markedly different (Fig. 2b, d), coercivity at 10 K for samples B and D are higher (>60 mT). These latter show open hysteresis loops but magnetic saturation is attained. Hysteresis loops are slightly wasp waisted which is an indication of a mixture of coercivity (Tauxe *et al*. 1996). But the most important feature of these specimens is the shift of hysteresis loop centre along the $+Y$ axis from 10 to 40 K. This shift is parallel to the applied field during the cooling of the sample.

We report in Fig. 3(a) the magnetization at saturation (M_s) inferred from hysteresis loops. M_s evolves differently for the two sets of claystones. M_s increases of more than 90 per cent for claystones A and C from 40 to 10 K. By contrast, the increase of M_s is less marked for claystones B and D. About 78 per cent of increase is observed. The same trends are observed for high field susceptibilities

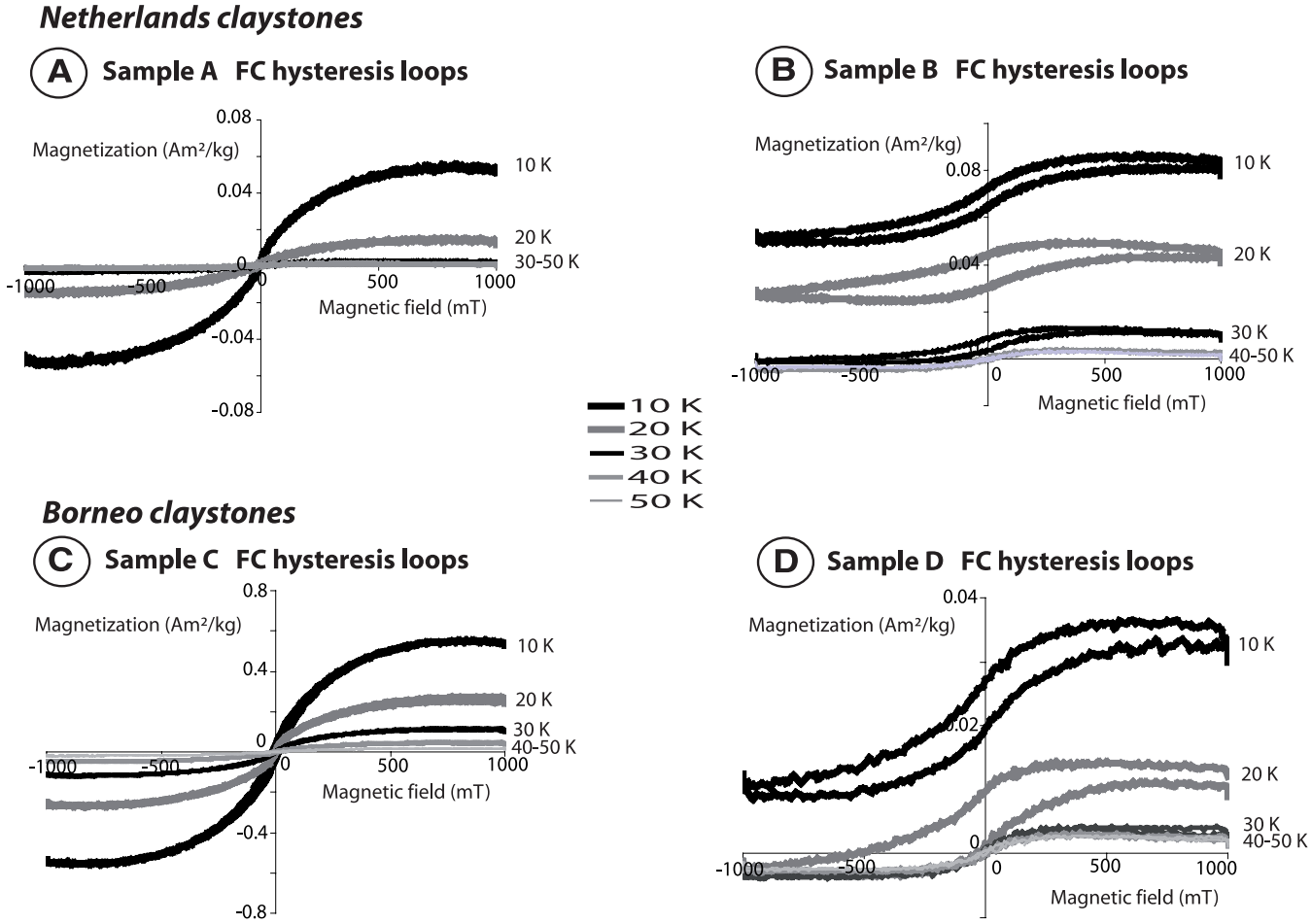

Figure 2. Field Cooled hysteresis loops from 50 K to 10 K for (a) sample A, (b) sample B from the Netherlands, and (c) sample C and (d) sample D from Borneo.

(X_{hf}; Fig. 3b). The X_{hf} of samples A and C increase of almost 70 per cent from 50 to 10 K, whereas the X_{hf} increase of sample D is smoother (45 per cent). The X_{hf} of sample B is quasi-stable.

We show in-phase (K') and out-out-phase (K'') AC susceptibility measurements in the 5–50 K temperature range (Fig. 3c, d). For the four claystones, we do not observe any field-dependency of K' and K''. In-phase K' shows different behaviour for the Netherlands claystones A and B (Fig. 3d). While K' regularly decreases from 10 to 50 K for sample A, a bump of K' is observed at ∼35 K for sample B. Out-of-phase K'' decreases in the same proportion from 10 to 50 K for both claystones A and B. It should be noted for sample A that (1) K'' is larger by one order of magnitude at 10 K compared to sample B, (2) there is a break-in-slope of K'' at ∼20 K. For Borneo claystones C and D, K' is decreasing from 10 to 50 K and it shows two break-in-slopes at ∼10 K and ∼20 K (Fig. 3d). The quadrature K'' of sample C displays a bump at ∼16 K. The magnitude of K'' is two times larger than that of sample D at 10 K.

4 DISCUSSION

Claystones A and C from the Netherlands borehole and the Borneo accretionary prism, respectively showed similar patterns as reported by Aubourg & Pozzi (2010). That consists in the recognition of *P*-behaviour, as well as the two-step pattern of ZFC curve, marked by a magnetic transition at ∼35 K and ∼120 K (Fig. 1). Both claystones experienced burial temperature T_{bu} less than 120°C, with respect to their vitrinite reflectance. However, the two other claystones, B and D, that both underwent $T_{bu} > 150$°C, do not show the *P*-behaviour. Instead, we observed Néel transition with a Néel temperature between 30 and 40 K. In the following, we attempt to distinguish the two types of samples.

4.1 Magnetite concentration

The concentration of magnetic grains can be approximated by using the SIRM value at room temperature. More precisely, the SIRM provides the concentration of ferromagnetic minerals capable to retain a remanence, that is, all grains above the blocking volume. The four samples present the Verwey transition at 120 K (Fig. 1), which is characteristic of the stoichiometric low coercive magnetite (Özdemir *et al*. 2002). The magnetic transition <50 K is carried by minerals that are paramagnetic or superparamagnetic at room temperature (e.g. Fe–Mn carbonates, iron sulphides). We assume therefore that magnetite constitutes the main magnetic mineral that carries the SIRM. To estimate the maximum magnetite concentration of the samples, we compare the SIRM to the half value of SIRM value of magnetite because magnetite minerals are not perfectly oriented (Aubourg *et al*. 2008). Using half value of magnetite SIRM at ∼10 $Am^2\ kg^{-1}$ (Maher *et al*. 1999) and the value of SIRM at room temperature (∼100 $\mu Am^2\ kg^{-1}$ to simplify), it

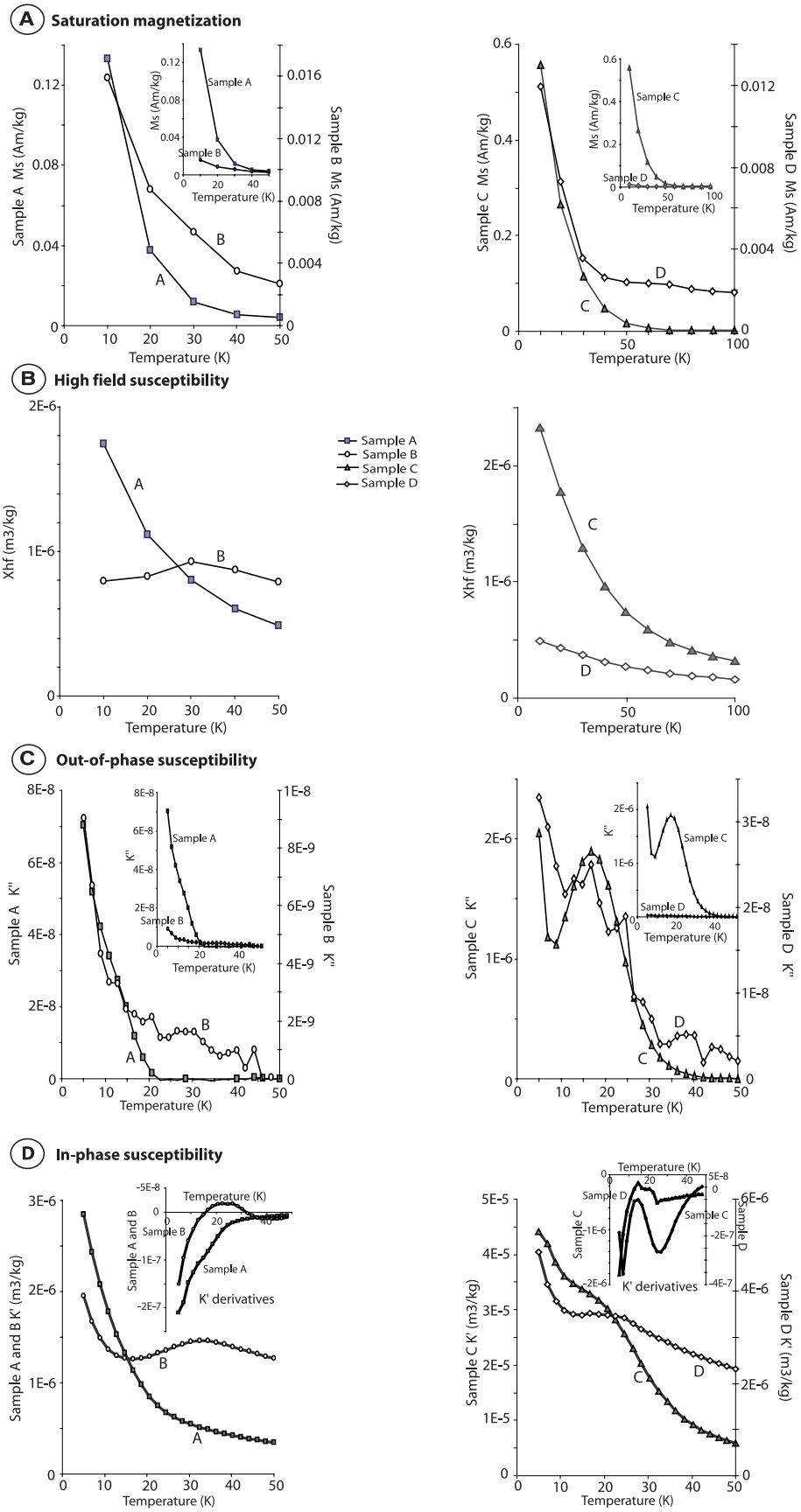

Figure 3. Evolution of (a) saturation magnetization, (b) high field susceptibility, 394 (c) Out-of-phase susceptibility and (d) in-phase susceptibility from 10 K to 50 K for the four claystones.

is found that the magnetite concentration is less than 10 ppm. The claystones contain therefore trace amount of magnetite above the blocking volume, that is, >20 nm. This low concentration of ferromagnetic mineral can be due to magnetite dissolution processes during burial (Rowan *et al*. 2009).

4.2 <50 K behaviours

In this study, we emphasized the <50 K magnetization evolution. In our protocol of RT-SIRM on cooling, the upward applied magnetic field of 5 μT inside the MPMS was found to be very useful to highlight the <50 K magnetic behaviour (Fig. 1b, d). In the following, we distinguished two classes: the *P*-class (samples A and C) and the *N*-class (samples B and D). Samples from the *P*-class display the *P*-behaviour, with progressive increase of an induced magnetization during the cooling of the RT-SIRM from ∼100 K (Fig. 1b, d). The slope of the derivative is regularly increasing down to 10 K. Samples from the *N*-class display abrupt Néel transition at 30 K and 38 K (Fig. 1b, d). The slope of the derivative is decreasing for temperature lower than 30 K.

For *P*-class and *N*-class samples, ZFC curves display the same 2-step pattern (Fig. 1a, c) and thus are not useful to distinguish between the two types of classes. Housen *et al*. (1996) noted already that ZFC curves of pyrrhotite, siderite and rhodochrosite displayed similar behaviours. Those are not so different from greigite SIRM warming curves (Chang *et al*. 2009). The best magnetic parameters to distinguish between *P*-class and *N*-class are the low-temperature hysteresis loops and the low temperature properties of magnetic susceptibility.

N-class samples display open FC hysteresis loops for T < 30 K (Fig. 2b, d). By contrast, the hysteresis loops of *P*-class samples remain narrow at low temperature (Fig. 2a, c). The most remarkable feature of *N*-class samples, however, is the observation of an offset of the hysteresis loops at 10 K and 20 K, characterized by a positive shift of the hysteresis loop along the axis of remanence (parallel to the field applied during cooling). By contrast, samples from the *P*-class do not show offset of hysteresis loops (Fig. 2a, c). The hysteresis loop offset was first reported by Housen *et al*. (1996) for siderite mineral. Kosterov *et al*. (2006) showed also offset of hysteresis loops for rhodochrosite.

Hysteresis parameters M_s (magnetization at saturation) and X_{hf} (high-field magnetic susceptibilities) show distinguishable differences (Fig. 3a, b). For the *P*-class samples, we observed an increase of more than 90 per cent of these parameters below 50 K. By contrast, the increase of M_s and X_{hf} is less marked for the *N*-class samples.

The low-temperature dependency of the in-phase (K') and out-of-phase (K'') AC magnetic susceptibilities provided additional information. Samples from the *N*-class displayed bumps of K' at ∼34 K for sample B and ∼22 K for sample D (Fig. 3d). Similar observations on siderite and rhodochrosite minerals are reported by Frederichs *et al*. (2003). Samples from the *P*-class displayed either no distinguishable bump during the decrease of K' (sample A) or break-in-slope for sample C (Fig. 3d). Out-of-phase K'' of *P*-class samples is one to two orders of magnitude larger than K'' of *N*-class samples. One way to explain the increase of K'' is the apparition of Foucault current in the mineral.

4.3 The nature of *P*-behaviour

Aubourg & Pozzi (2010) proposed that the *P*-behaviour observed during cooling of a RT-SIRM is carried by fine-grained pyrrhotite. However occurrence of this mineral needs further analysis and the *P*-behaviour can be a form of Néel transition of siderite ($T_N = 38$ K) and/or rhodochrosite ($T_N = 32$ K). Unlike *P*-class samples which exhibit *P*-behaviour, the *N*-class samples displayed unambiguous Néel temperature of ∼38 K for sample B and ∼30 K for sample D. These temperatures correspond respectively to siderite and rhodochrosite Néel transitions. Recognition of hysteresis loops offset (Fig. 2b, d) is an additional evidence of the occurrence of siderite and rhodochrosite (Housen *et al*. 1996; Kosterov *et al*. 2006).

It is possible that the *P*-behaviour is a combination of rhodochrosite/siderite transition and an input of an additional magnetic mineral. Sample A is possibly the illustration of this combination. From the derivative of the RT-SIRM on cooling, we observed a break-in-slope at ∼30 K (Fig. 1b). Thus the *P*-behaviour in this case is possibly triggered by the input of rhodochrosite. However, hysteresis loops do not show any offset nor opening at low-temperature (Fig. 2a, c). The sample C does not show evidence of Néel temperature between 30 and 38 K (Fig. 1d). We do not think that sample C *P*-behaviour is due to rhodochrosite/siderite for additional reasons. The *P*-behaviour is not abrupt, as it should be for a Néel transition (e.g. sample D in Fig. 1d). We do not observe shift of hysteresis loops at low temperature (Fig. 2c). There is a large increase by one to two orders of magnitude of the remanence at saturation, the high-field magnetic susceptibility and the out-of-phase magnetic susceptibility for the *P*-class samples.

4.4 <50 K behaviours and maturity of rocks

Aubourg & Pozzi (2010) proposed that *P*-behaviour develops at ∼60°C from the basis of experimental studies and natural observation. Ongoing studies by our group demonstrate the large occurrence of *P*-behaviour in immature to early mature claystones ($T_{bu} < 120$°C). The early mature claystone C from Borneo is an additional evidence for the development of the *P*-behaviour. However, for overmature claystones B and D ($T_{bu} > 150$°C; Ro > 1.2 per cent), we observed the development of a Néel transition of siderite and rhodochrosite. For calcareous claystone A, the *P*-behaviour is probably carried by rhodochrosite. Rhodochrosite and siderite occur in rapidly accumulating, fine-grained, organic rich sediment (Glasby & Schulz 1999). Rhodochrosite is observed at very low-grade metamorphic condition and is stable at higher grade (Peters *et al*. 1973). Further work is necessary to see if the Néel transitions of overmature claystones ($T_{bu} > 150$°C) is a marker of low-grade metamorphism or if it is related to the sedimentary conditions.

5 CONCLUSION

We performed magnetic measurements to characterize the magnetic assemblage of four early mature to overmature claystones from a borehole in the Netherlands and from Borneo prism. We focused on the <50 K magnetic behaviour. To evidence Néel transition, we applied a magnetic field of 5 μT inside the SQUID MPMS during the cooling of a SIRM. We proposed two classes of samples: the *P*-class and the *N*-class. Both classes contain magnetite in trace amount (<10 ppm). In the *P*-class, during the cooling of a SIRM, we observed an increase of induced magnetization at ∼100 K, named *P*-behaviour. The *P*-behaviour may be a fingerprint of early mature claystones ($T_{bu} < 120$°C) and might be carried by iron sulphides and possibly by the contribution of Néel-type mineral like siderite or rhodochrosite. In addition, the *P*-class samples showed enhancement below 50 K by one to two orders of magnitude of the

magnetization at saturation, the high-field magnetic susceptibility and the out-of-phase magnetic susceptibility. The *N*-class samples, where claystones are overmature ($T_{bu} > 150°C$), showed Néel transitions at 30 K and 38 K that suggest the occurrence of rhodochrosite and siderite. The offset of field-cooled hysteresis loops and the increase of the coercivity for T < 30 K comforted the hypothesis of the occurrence of rhodochrosite and siderite. Further work is necessary to confirm our hypothesis that the *P*-class and *N*-class claystones are correlated to the index maturity of claystones; immature to mature for the *P*-class (T_{bu}∼60–<120°C), and overmature ($T_{bu} > 150°C$) for the *N*-class. If correct, the low-temperature magnetic investigation will constitute a valuable tool to precise very low-grade metamorphism of claystones.

ACKNOWLEDGMENTS

This work was conducted as a part of M. Kars PhD. Thesis supported by Total S.A./Université de Pau et des Pays de l'Adour, France.
We are grateful to IRM for providing us instrumental facilities and for invaluable discussions. F. Sapin and M. Pubellier provided us claystones from Borneo. We benefited from a grant from the University of Minnesota for our 10-day visit at the IRM in 2009.
We would like to thank reviewers Andrei Kosterov and Pierre Rochette, and editor Cor Langereis for their accurate comments.

REFERENCES

Aubourg, C. & Pozzi, J-P., 2010. Toward a new <250°C pyrrhotite-magnetite geothermometer for claystones, *Earth planet. Sci. Lett.*, **294**(1–2), 47–57.

Aubourg, C., Pozzi, J-P. Janots, D., & Sahraoui, L., 2008. Imprinting chemical remanent magnetization in claystones at 95°C, *Earth planet. Sci. Lett.*, **272**, 172–180.

Chang, L., Roberts, A.P., Rowan, C. J., Tang, Y. Pruner, P. Chen, Q., & Horng, C-S., 2009. Low-temperature magnetic properties of greigite (Fe_3S_4), *Geochem. Geophys. Geosyst.*, **10**(1), Q01Y04, doi:10.1029/2008GC002276.

Dekkers, M.J., Mattei, J-L. Fillion, G., & Rochette, P., 1989. Grain size dependence of magnetic behavior of pyrrhotite during its low-temperature transition at 34 K, *Geophys. Res. Lett.*, **16**, 855–858.

Frederichs, T., von Dobeneck, T. Bleil, U. & Dekkers, M.J., 2003. Towards the identification of siderite, rhodochrosite and vivianite in sediments by their low-temperature magnetic properties, *Phys. Chem. Earth*, **28**, 669–679.

Glasby, G.P. & Schulz, H.D., 1999. E_H, pH diagrams for Mn, Fe, Co, Ni, Cu and As under seawater conditions: application of two new types of E_H, pH diagrams to the study of specific problems in marine geochemistry, *Aqua. Geochem.*, **5**, 227–248.

Hirt, A.M., Lanci, L., Dobson, J. Weidler, P. & Gehring, A.U., 2002. Low-temperature magnetic properties of lepidocrocite, *J. geophys. Res.*, **107**(B1), 2011, doi:10.1029/2001JB000242.

Housen, B.A., Banerjee, S.K. & Moskowitz, B.M., 1996. Low-temperature magnetic properties of siderite and magnetite in marine sediments, *Geophys. Res. Lett.*, **23**(20), 2843–2846.

Kosterov, A., Frederichs, T. & von Dobeneck, T., 2006. Low-temperature magnetic properties of rhodochrosite (MnCO3), *Phys. Earth planet. Inter.*, **154**, 234–242.

Maher, B.A., Thompson, R. & Hounslow, M.W., 1999. Introduction to quaternary climates, environments and magnetism, in *Quaternary Climates, Environments and Magnetism*, pp. 1–48, eds Maher, B.A. & Thompson, R., Cambridge University Press, Cambridge.

Muxworthy, A.R. & McClelland, E. 2000. Review of the low-temperature magnetic properties of magnetite from a rock magnetic perspective, *Geophys. J. Int.*, **140**, 101–114.

Ozdemir, O., Dunlop, D.J. & Moskowitz, B.M., 2002. Changes in remanence, coercivity and domain state at low temperature in magnetite, *Earth planet. Sci. Lett.*, **194**(3–4), 343–358.

Peters, T., Schwander, H. & Trommsdorff, V., 1973. Assemblages among tephroite, pyroxmangite, rhodochrosite, quartz: experimental data and occurrences in the Rhetic Alps, *Contrib. Mineral. Pet.*, **42**, 325–332.

Rochette, P., Fillion, G. Mattei, J-L. & Dekkers,M.J., 1990. Magnetic transition at 30–40 Kelvin in pyrrhotite insight into a widespread occurrence of this mineral in rocks, *Earth planet. Sci. Lett.*, **98**, 319–328.

Rowan, C.J., Roberts, A.P. & Broadbent, T., 2009. Reductive diagenesis, magnetite dissolution, greigite growth and paleomagnetic smoothing in marine sediments: a new view, *Earth planet. Sci. Lett.*, **277**, 223–235.

Sapin, F., Pubellier, M., Lahfid, A., Janots, D. Aubourg, C. & Ringenbach, J.C., 2011. Onshore record of the subduction of a crustal salient : example of the NW Borneo Wedge, *Terra Nova*, **23,** 232–240.

Sweeney, J.J & Burnham, A.K., 1990. Evaluation of a simple model of vitrinite reflectance based on chemical kinetics, *AAPG Bull.*, **74**(10), 1559–1570.

Tauxe, L., Mullender, T.A.T. & Pick, T. 1996. Potbellies, wasp-waists and superparamagnetism in magnetic hysteresis, *J. geophys. Res.*, **101**(B1), 571–583.

Van Velzen, A.J. & Zijderveld, J.D.A., 1992. A method to study alterations of magnetic minerals during thermal demagnetization applied to a fine-grained marine marl (Trubi formation, Sicily), *Geophys. J. Int.*, **110**(1), 79–90.

Walz, F., 2002. The Verwey transition – a topical review, *J. Phys. Condens. Matter*, **14**, R285–R340.